0026-895X/98/010062-15$3.00/0

MOLECULAR PHARMACOLOGY, **53**:62–76 (1998).

Structure-Activity Analysis of the Interaction of Curacin A, the Potent Colchicine Site Antimitotic Agent, with Tubulin and Effects of Analogs on the Growth of MCF-7 Breast Cancer Cells

PASCAL VERDIER-PINARD, JING-YU LAI, HAE-DONG YOO, JURONG YU, BRIAN MARQUEZ, DALE G. NAGLE, MITCH NAMBU, JAMES D. WHITE, J. R. FALCK, WILLIAM H. GERWICK, BILLY W. DAY, and ERNEST HAMEL

Laboratory of Drug Discovery Research and Development, Developmental Therapeutics Program, Division of Cancer Treatment, and Diagnosis, National Cancer Institute, Frederick Cancer Research and Development Center, Frederick, Maryland 21702 (P.V.-P., E.H.), Departments of Biochemistry and Pharmacology, Southwestern Medical Center, The University of Texas at Dallas, Dallas, Texas 75235 (J.Y.L., J.Y., J.R.F.), College of Pharmacy, Oregon State University, Corvallis, Oregon 97331 (H.-D.Y., B.M., D.G.N., W.H.G.), Department of Chemistry, Oregon State University, Corvallis, Oregon 97331 (M.N., J.D.W.), and Departments of Environmental and Occupational Health and of Pharmaceutical Sciences, University of Pittsburgh Cancer Institute, University of Pittsburgh, Pittsburgh, Pennsylvania 15238 (B.W.D.)

Received March 26, 1997; Accepted September 15, 1997

ABSTRACT

Originally purified as a major lipid component of a strain of the cyanobacterium *Lyngbya majuscula* isolated in Curaçao, curacin A is a potent inhibitor of cell growth and mitosis, binding rapidly and tightly at the colchicine site of tubulin. Because its molecular structure differs so greatly from that of colchicine and other colchicine site inhibitors, we prepared a series of curacin A analogs to determine the important structural features of the molecule. These modifications include reduction and *E*-to-*Z* transitions of the olefinic bonds in the 14-carbon side chain of the molecule; disruption of and configurational changes in the cyclopropyl moiety; disruption, oxidation, and configurational reversal in the thiazoline moiety; configurational reversal and substituent modifications at C13; and demethylation at C10. Inhibitory effects on tubulin assembly, the binding of colchicine to tubulin, and the growth of MCF-7 human breast carcinoma cells were examined. The most important portions of curacin A required for its interaction with tubulin seem to be the thiazoline ring and the side chain at least through C4, the portion of the side chain including the C9–10 olefinic bond, and the C10 methyl group. Only two modifications totally eliminated the tubulin-drug interaction. The inactive compounds were a segment containing most of the side chain, including its two substituents, and analogs in which the methyl group at the C13 oxygen atom was replaced by a benzoate residue. Antiproliferative activity comparable with that observed with curacin A was only reproduced in compounds that were potent inhibitors of the binding of colchicine to tubulin. Molecular modeling and quantitative structure-activity relationship studies demonstrated that most active analogs overlapped extensively with curacin A but failed to provide an explanation for the apparent structural analogy between curacin A and colchicine.

Antimitotic agents, both natural products and synthetic compounds, display a wide structural diversity, and virtually all of them interact with the α/β-tubulin dimer, the major component of microtubules (Hamel, 1990, 1996). Most of these compounds inhibit microtubule assembly in cells and in cell-free systems. A major mechanism involved in the cytotoxic action of these drugs seems to be altered microtubule dynamics, and most drugs studied thus far reduce tubulin turnover at microtubule ends. Thus, antimitotic agents may inhibit mitosis primarily by stabilizing the (+)-ends of microtubules in the spindle (Wilson and Jordan, 1995).

Net inhibitors of microtubule assembly largely fall into two classes. The first group consists of a variety of complex natural products that inhibit the binding of vinca alkaloids to tubulin, inhibit formation of an intra-β-tubulin cross-link between Cys12 and Cys201/211, and interfere with GTP/GDP exchange on β-tubulin (vinca domain agents). The second group consists of numerous synthetic compounds and structurally simpler natural products, such as the *cis*-stilbene combretastatin A-4 and the estrogen metabolite 2-methoxyestradiol (see representative structures in Fig. 1). These compounds inhibit the binding of colchicine to tubulin, inhibit formation of an intra-β-tubulin cross-link between Cys239 and Cys354, have no effect on GTP/GDP exchange,

ABBREVIATIONS: HPLC, high performance liquid chromatography; GC, gas chromatography; EIMS, electron ionization mass spectrometry; QSAR, quantitative structure-activity relationship(s) CHARMm, chemistry at Harvard macromolecular mechanics; MOPAC, molecular orbital package; CNDO, complete neglect of differential overlap; MNDO, modified neglect of differential overlap.

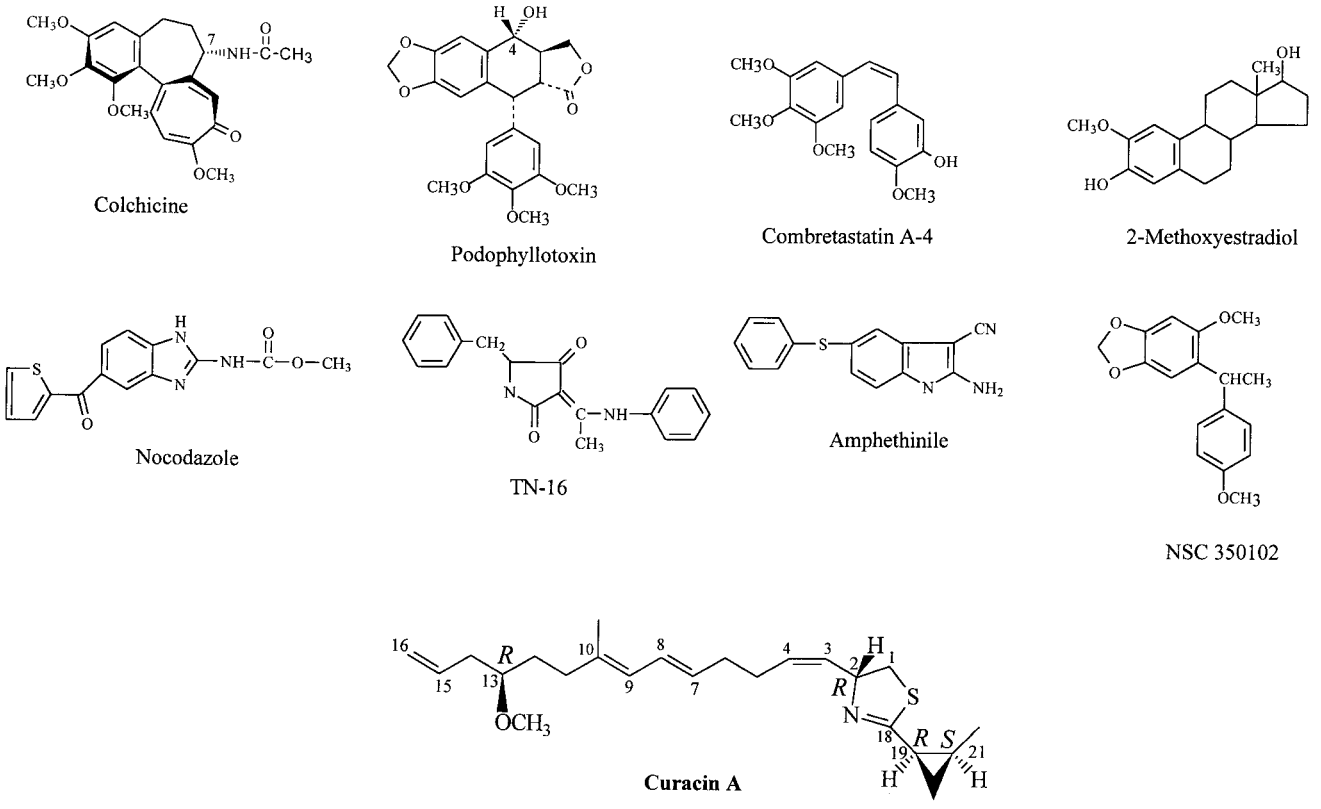

Fig. 1. Structural formulas of antimitotic compounds, including curacin A, that bind in the colchicine site of tubulin.

and generally induce a GTPase reaction uncoupled from assembly (colchicine site agents). A recurring structural theme in the colchicine site agents has been at least one and generally two aromatic domains (for reviews, see Hamel, 1996, and Ludueña and Roach, 1991).

Curacin A (structure in Fig. 1; see Nagle *et al.*, 1995), as a potent colchicine site antimitotic agent, is a major exception to this structural generalization, in that it has no aromatic residue. Curacin A is a major lipid component of a strain of *Lyngbya majuscula* obtained off the coast of Curaçao (Gerwick *et al.*, 1994). The compound inhibits microtubule assembly and, despite its unique structure, is a potent competitive inhibitor of the binding of colchicine to tubulin (Blokhin *et al.*, 1995). Initial studies demonstrated that curacin A stimulated the uncoupled GTPase reaction typical of colchicine site agents, and indirect observations were consistent with curacin A binding rapidly and dissociating slowly from tubulin (Blokhin *et al.*, 1995). Further, curacin A inhibits formation of the Cys239-Cys354 cross-link in β-tubulin (Ludueña *et al.*, 1997). Moreover, under reaction conditions where tubulin can polymerize, high concentrations of curacin A induced formation of complex abnormal tubulin polymers resembling twisted cables of fine spiral filaments (Hamel *et al.*, 1995). Curacin A may also have a relatively unusual effect on microtubule dynamics, in that low concentrations of the drug increase tubulin turnover at microtubule ends (Pack *et al.*, 1995).

The unusual structure and unexpected biological activity of curacin A led to the rapid development of successful chemical syntheses (Hoemann *et al.*, 1996; Ito *et al.*, 1996; Lai *et al.*, 1996; Onoda *et al.*, 1996a, b; White *et al.*, 1995, 1997; Wipf and Xu, 1996), and the abundance of the natural product has permitted isolation of chemically modified derivatives. In addition, small quantities of related compounds have been isolated from natural sources [curacins B and C from the Curaçao strain of *L. majuscula* (Yoo and Gerwick, 1995) and curacin D from a St. Thomas (US Virgin Islands) strain of *L. majuscula*]. Initial structure-activity findings have already been reported (Blokhin *et al.*, 1995; Onoda *et al.*, 1996b), but a sufficient variety of analogs is now available to permit a more systematic analysis of the structural features of the curacin A molecule required for its interaction with purified tubulin. We also report relative effects of available compounds on the growth of a human breast cancer cell line (MCF-7 cells).

Experimental Procedures

Materials

Electrophoretically homogeneous bovine brain tubulin was prepared as described previously (Hamel and Lin, 1984). Nonradiolabeled colchicine was obtained from Sigma (St. Louis, MO) and [^{3}H]colchicine from Dupont-New England Nuclear (Boston, MA). Stock 2.0 M solutions of monosodium glutamate were adjusted to pH 6.6 with HCl. MCF-7 breast cancer cells were a generous gift from Dr. D. Scudiero (National Cancer Institute, Frederick, MD). Curacins A, B, and C from *L. majuscula* were obtained as described previously (Gerwick *et al.*, 1994; Yoo and Gerwick, 1995). Synthetic curacin A (Lai *et al.*, 1996) had activity equivalent to the natural product, and all data presented for curacin A represent averages obtained in contemporaneous experiments with natural and synthetic drug. Synthetic analogs are assigned numbers in the order in which they will be presented in Results. Compounds **1** (15, 16-dihydrocuracin A), **12** (19*S*-curacin A), **14** ("cyclopropyl-ring-open-curacin A"), and **22** were prepared as described previously (Blokhin *et al.*, 1995; White *et al.*, 1997). The isolation of curacin D will be

described elsewhere, as will the synthesis of compounds **3**-**9**, **13**, and **15**-**21**. All drugs were dissolved in dimethyl sulfoxide, and control reaction mixtures contained an equivalent amount of the solvent.

Preparation of 3,4,15,16-Tetrahydrocuracin A (Compound 2)

$[(C_6H_5)_3P]_3RhCl$ (11.3 mg, 12.2 μmol) in 0.50 ml CH_2Cl_2 was added to curacin A (49 mg, 131 μmol) in 0.50 ml ethanol. An additional 2.5 ml of CH_2Cl_2 was added, and the reaction flask, with an attached balloon, was charged with H_2. After 7 hr at room temperature, 40 ml of a 1:1 mixture of ethanol and diethyl ether was added to the reaction mixture, and the catalyst was removed by filtration through a silica plug. Pure compound **2** was obtained from the filtrate by HPLC on a Maxsil 10 μm silica column (50 × 1.0 cm; Phenomenex, Torrance, CA) using 4% (v/v) ethyl acetate in hexanes (eluted at 680–730 ml). The chemical characterization of compound **2** is as follows: [^{1}H NMR (C_6D_6, 300 MHz) δ 6.40 (dd, 1H, J = 14.9, 11.1, H-8), 6.01 (d, 1H, J = 11, H-9), 5.65 (m, 1H, H-7), 4.15 (m, 1H, H-2), 3.18 (s, 3H, -OCH_3), 3.08 (m, 1H, H-13), 2.90 (dd, 1H, J = 10.8, 8.3, H-1b), 2.60 (dd, 1H, J = 10.2, 9.8, H-1a), 2.15 (m, 2H, H-11), 2.13 (m, 2H, H-6), 1.70 (s, 3H, H-17), 1.69–1.51 (m, 3H, H-12 and H-19), 1.5–1.3 (m, 10H, H-3, H-4, H-5, H-14, and H-15), 1.2 (m, 1H, H-20b), 1.18 (d, 3H, J = 6.3, H-22), 0.95 (m, 1H, H-21), 0.9 (m, 3H, H-16), 0.75 (m, 1H, H-20a); GC EIMS (% rel. int.) obs. $[M]^+$ m/z 377 (65), 362 $[M - CH_3]^+$ (36), 346 $[M - OCH_3]^+$ (29), 334 $[M - C_3H_7]^+$ (11), 302 (11), 290 $[M - C_5H_{11}O]^+$ (33), 276 $[M - C_6H_{13}O]^+$ (83), 262 $[M - C_7H_{15}O]^+$ (15), 234 (18), 222 (10), 208 (29), 194 (17), 182 $[C_{10}H_{16}NS]^+$ (17), 180 $[M - C_{13}H_{23}O]^+$ (16), 176 (33), 168 $[C_8H_{12}NS]^+$ (18), 166 (28), 154 $[C_8H_{12}NS]^+$ (33), 141 (60), 140 $[C_7H_{10}NS]^+$ (100), 113 (31), 107 (25), 105 (33), 99 $[C_5H_7S]^+$ (36), 93 (45), 91 (40), 87 $[C_5H_{11}O]^+$ (47), 81 (40), 79 (51), 67 $[C_5H_7]^+$ (28), 55 $[C_4H_7]^+$ (39)].

Preparation of [13*R*,19*R*,21*S*]-1,2-Didehydrocuracin A (Compound 10; "Curazole")

MnO_2 (200 mg, 2.3 mmol) was added to 2.0 ml of hexanes containing curacin A (17.6 mg, 47 μmol). The stirred reaction at 25° was monitored by thin layer chromatography. After 5 days, the MnO_2 was removed by filtration and washed with hexanes. The wash was added to the filtrate and the solvent removed under vacuum. The residue was dissolved in 2% (v/v) ethyl acetate in hexanes. HPLC purification was on a Versapack 10 μm silica column (30 × 0.41 cm; Alltech, Deerfield, IL), developed at 2.0 ml/min with 2% (v/v) ethyl acetate in hexanes. The chemical characterization of compound **10** (colorless oil, 5 mg, 13.5 μmol, 29% yield) is as follows: IR ν_{max} (film) 3017, 2924, 2851, 1640, 1617, 1505, 1439, 1385, 1354, 1084, 964, 914, 779 cm^{-1}; UV λ_{max} (ethanol) 224 nm (log ε, 4.43), 242 nm (log ε, 4.49), 252 nm (log ε, 4.42); [^{1}H NMR (C_6D_6, 400 MHz) δ 6.46 (s, 1H, H-1), 6.44 (bd, 1H, J = 11.7, H-3), 6.40 (bdd, 1H, J = 15.2, 10.9, H-8), 5.97 (bd, 1H, J =10.9, H-9), 5.83 (ddt, 1H, J = 17.0, 10.2, 7.3, H-15), 5.68 (dt, 1H, J = 11.7, 7.3, H-4), 5.66 (bd, 1H, J = 15.2, H-7), 5.02 (m, 2H, H-16), 3.13 (s, 3H, -OCH_3), 3.04 (tt, 1H, J = 6.0, 6.0, H-13), 2.89 (bdt, 2H, J = 7.4, 6.0, H-5), 2.30 (m, 2H, H-6), 2.19 (m, 2H, H-14), 2.13 (m, 2H, H-11), 2.00 (dt, 1H, J = 8.1, 5.2, H-19), 1.67 (s, 3H, H-17), 1.60 (m, 2H, H-12), 1.13 (m, 1H, H-20b), 1.05 (d, 3H, J = 6.0, H-22), 0.95 (m, 1H, H-21), 0.86 (ddd, 1H, J = 8.1, 5.2, 4.3, H-20a)]; [^{13}C NMR (C_6D_6, 100 MHz) δ 168.68 (C18), 153.88 (C2), 136.00 (C10), 135.58 (C15), 133.02 (C4), 131.97 (C7), 127.76 (C8), 125.73 (C9), 122.90 (C3), 116.72 (C16), 115.26 (C1), 79.99 (C13), 56.30 (-OCH_3), 38.07 (C14), 35.78 (C11), 33.35 (C6), 32.15 (C12), 29.58 (C5), 19.85 (C19), 16.57 (C17), 16.47 (C21), 14.94 (C20), 12.66 (C22); GC EIMS (% rel. int.) obs. $[M]^+$ m/z 371 (11), 356 $[M - CH_3]^+$ (29), 340 $[M - OCH_3]^+$ (26), 330 (18), 298 (21), 286 (36), 272 (37), 258 (11), 230 (11), 204 (24), 178 (81), 161 (30), 153 (50), 133 (17), 119 (76), 105 (53), 97 (100), 91 (51) 79 (64), 67 (35), 55 (25)].

Preparation of Compound 11 ("Thiazole-Ring-Open-Curacin A")

Curacin A (18 mg, 48.3 μmol) was dissolved in 1.5 ml of acetic anhydride containing 3 drops of D_2O. The reaction mixture was stirred and left overnight at room temperature. After solvent removal under vacuum, the residue was suspended in 25% (v/v) ethyl acetate in hexanes and passed through sintered glass. The filtrate was chromatographed on a Phenomenex Maxil 10 μm silica HPLC column (50 × 1.0 cm), which was developed at 9 ml/min with 25% (v/v) ethyl acetate in hexanes. The chemical characterization of compound **11** (7.6 mg, 17.6 μmol, 42% yield) is as follows: IR ν_{max} (film) 3270, 2929, 1678, 1650, 1547, 1536, 1435, 1371, 1096, 963, 913 cm^{-1}; $[\alpha]_D^{22}$ +58° (c0.1, $CHCl_3$); UV λ_{max} (methanol) 240 nm (log ε, 4.49); [^{1}H NMR (C_6D_6, 300 MHz) δ 6.42 (dd, 1H, J = 15.0, 10.8, H-8), 6.02 (d, 1H, J = 10.8, H-9), 5.87 (m, 1H, H-15), 5.62 (dt, 1H, J = 15.0, 10.0, H-7), 5.48 (dt, 1H, J = 10.5, 7.1, H-4), 5.2 (dd, 1H, J = 10.5, 9.0, H-3), 5.10 (m, 1H, H-2), 5.07 (m, 2H, H-16), 3.18 (s, 3H, -OCH_3), 3.09 (m, 1H, H-13), 3.04 (m, 2H, H-1), 2.35 (m, 2H, H-5), 2.26 (m, 2H, H-14), 2.23 (m, 2H, H-11), 2.11 (m, 2H, H-6), 1.8 (m, 1H, H-19), 1.7 (s, 3H, H-17), 1.65 (m, 2H, H-12), 1.58 (s, 3H, CH_3CO), 1.12 (d, 3H, J = 6.1, H-22), 1.11 (m, 1H, H-20b), 0.96 (m, 1H, H-21), 0.66 (m, 1H, H-20a)]; [^{13}C NMR (C_6D_6, 75 MHz) δ 196.95 (C18), 167.99 (CH_3CONH), 136.19 (C10), 135.37 (C15), 132.89 (C4), 131.58 (C7), 129.21 (C3), 127.0 (C8), 125.64 (C9), 116.75 (C16), 79.95 (C13), 56.29 (-OCH_3), 47.40 (C2), 38.05 (C14), 35.77 (C11), 33.59 (C1), 33.09 (C6), 32.14 (C12), 28.16 (C5), 22.97 (C19), 19.39 (C21), 16.60 (C17), 16.15 (C20), 11.95 (C22); GC EIMS (% rel. int.) obs. $[M]^+$ m/z 433 (1), 318 (4), 259 (4), 200 (5), 185 (5), 161 (10), 119 (20), 111 (11), 105 (18), 91 (19), 85 (21), 84 (34), 83 (100), 79 (20), 55 (22); HR FAB MS (positive) obs. [M + H]$^+$ at m/z 434.2728 ($C_{25}H_{40}NO_3S$, deviation of - 0.1 milliatomic mass units)].

Preparation of Compound 23 (Methylthioether Derivative of Curacin A)

A solution of compound **11** (7.0 mg, 19 μmol) in 2.0 ml of dry tetrahydrofuran was added to 1.0 μl (34.1 μmol) of CH_3Li at −78°. After 1.5 hr, 1.3 μl (20.4 μmol) of CH_3I was added, and the reaction mixture was stirred for 1 hr at −78°. After solvent removal under vacuum, the residue was suspended in ethyl acetate and passed through sintered glass. The filtrate was chromatographed on a Phenomenex Maxil 10 μm silica HPLC column (50 × 1.0 cm), which was developed at 9 ml/min with ethyl acetate. The initial peak eluted from the column was rechromatographed with 30% (v/v) ethyl acetate in hexanes to yield compound **23** (0.4 mg, 1.1 μmol, 5.7% yield). The chemical characterization of compound **23** is as follows: [^{1}H NMR (C_6D_6, 300 MHz) δ 6.40 (dd, 1H, J = 14.9, 10.7, H-8), 6.02 (d, 1H, J = 10.7, H-9), 5.88 (m, 1H, H-15), 5.60 (m, 1H, H-7), 5.52 (m, 1H, H-4), 5.19 (dd, 1H, J = 10.4, 9.0, H-3), 5.10 (m, 2H, H-16), 5.10 (m, 1H, H-2), 4.70 (br, 1H, NH), 3.18 (s, 3H, -OCH_3), 3.09 (m, 1H, H-13), 2.46 (d, 2H, J = 5.8, H-1), 2.40 (m, 2H, H-5), 2.25 (m, 4H, H-11 and H-14), 2.18 (m, 2H, H-6), 1.91 (s, 3H, -SCH_3), 1.69 (s, 3H, H-17), 1.65 (m, 2H, H-12), 1.55 (s, ^{3}H, CH_3CO)]; [^{13}C NMR (DEPT 135°, C_6D_6, 75 MHz) δ 135.37, 132.88, 131.43, 129.51, 127.67, 125.56, 116.81, 79.96, 56.32, 45.70, 39.89, 38.06, 35.80, 33.12, 32.16, 28.31, 22.94, 16.62, 15.89; GC EIMS (% rel. int.) obs. $[M]^+$ m/z 365 (1), 333 (12), 318 (2), 304 (1), 234 (9), 227 (14), 213 (25), 207 (18), 185 (38), 171 (22), 161 (73), 159 (43), 145 (40), 133 (46), 119 (100), 117 (48), 111 (55), 105 (92), 94 (32), 85 (89), 77 (42), 69 (66), 55 (47)].

Chemical Methods

NMR spectra were recorded on AM 400 and AC 300 spectrometers (Bruker, Karlsruhe, Germany). Chemical shifts were referenced to the solvent C_6D_6 signals at 7.2 ppm for ^{1}H NMR and at 128 ppm for ^{13}C NMR. Mass spectra were recorded on Kratos (Manchester, England) MS 50 TC and Finnigan (San Jose, CA) 4023 mass spectrometers. Gas chromatography/mass spectrometry was carried out utilizing a Hewlett-Packard 5890 Series II gas chromatograph connected to a Hewlett-Packard 5971 mass selective detector (Hewlett-Packard, Palo Alto, CA). UV and IR spectra were obtained, respectively, on Hewlett-Packard 8452A and Nicolet 510 spectrophotometers (Nicolet, Madison, WI).

Biological Methods

The binding of [^{3}H]colchicine to tubulin was measured by the DEAE-cellulose filter method as described previously (Kang *et al.*, 1990). Reaction mixtures contained 1.0 μM (0.1 mg/ml) tubulin, 1.0 M monosodium glutamate, 0.1 M glucose-1-phosphate, 1.0 mM $MgCl_2$, 1.0 mM GTP, 0.5 mg/ml bovine serum albumin, 5% (v/v) dimethyl sulfoxide, 5.0 μM [^{3}H]colchicine, and inhibitor at either 5.0 or 50 μM, as indicated. These reaction conditions were used because they strongly stabilize the colchicine binding activity of tubulin (Hamel and Lin, 1981). The values presented represent averages of three experiments, each with duplicate samples.

Tubulin polymerization was followed turbidimetrically at 350 nm in Gilford (Oberlin, OH) model 250 spectrophotometers equipped with electronic temperature controllers. All concentrations refer to the final reaction volume of 0.25 ml, although the preincubation was performed in 0.24 ml, followed by addition of 10 μl of 10 mM GTP. Reaction mixtures contained 1.0 mg/ml tubulin, 0.8 M monosodium glutamate, 4% dimethyl sulfoxide, and varying drug concentrations. Samples were preincubated for 15 min at 30° and chilled on ice. GTP was added to each reaction mixture, and these were placed in cuvettes held at 0°. Base-lines were established, the temperature was raised to 30° (about 0.5°/sec), and polymerization was followed for 20 min. IC_{50} values were determined by graphical interpolation of experimental points, with drug-containing samples compared with control reaction mixtures containing dimethyl sulfoxide but no drug. At least three independent IC_{50} values were obtained with each compound.

IC_{50} values for inhibition of cell growth were obtained by measuring the amount of total cell protein with the sulforhodamine B assay (Skehan *et al.*, 1990). MCF-7 cells were grown in RPMI 1640 medium containing 17% fetal calf serum, 12 μg/ml gentamicin sulfate, and 2 mM glutamine at 37° in 5% CO_2. Confluent cells were trypsinized, diluted 40-fold, and seeded into 96-well microtiter plates. After 24 hr of growth without drug, medium with varying concentrations of drug was added to different wells (final concentration of dimethyl sulfoxide, 0.1%). IC_{50} values were determined after an additional 48 hr. The values presented in the tables are averages from at least two independent experiments.

Accumulation of MCF-7 cells with G2/M DNA content was quantified by flow cytometry. Cells were grown as described above, except that 25-ml cultures were grown in 75-cm^2 flasks, and the cells were trypsinized after 48 hr of drug treatment. A portion of the cells in each culture was quantified in a model ZM Coulter Counter (Coulter Products, Buffalo, NY). The remaining cells were collected by centrifugation, resuspended in phosphate-buffered saline (10 mM phosphate, 155 mM NaCl, pH 7.4) and fixed in 70% ethanol for 30 min at 4°. The cells were recollected by centrifugation and resuspended in 1 ml of phosphate-buffered saline containing 100 μg each of propidium iodide and RNase A. DNA content was analyzed on a FACScan flow cytometer, and the proportion of cells in G2/M quantified by peak integration using ModFit LT version 1.0 software (Becton Dickinson, Mountain View, CA).

Molecular Modeling Studies

Computational methods. Three-dimensional computer models of the curacins were built with the Cerius^2 system (version 2.0; Biosym/Molecular Simulations, Burlington, MA), run on an Iris Indigo/R3000 workstation (Silicon Graphics, Mountain View, CA) with Elan graphics running under the Irix 5.3 operating system. The molecular model of curacin A was built and minimized with CHARMm using the Merck Molecular Force Field by the conjugate gradient and adopted-basis Newton-Raphson methods in a constant dielectric field of 1. All 30° bond angle conformers of this model were analyzed by the grid scan method with 500 steps of conjugate gradient minimization, and a "global" minimum model was selected. This model was used as a template for developing models for the 26 congeners, which were each minimized by the same molecular mechanics methods.

Calculation of descriptors. Structures were superimposed on the most active analogs in the biological assays by rigid fit of subgraph searches, and receptor models were generated with the associated biological activity of each structure (IC_{50} values transformed to their negative base 10 logarithms) used as the weight by which it contributed to the model. Electronic, shape, spatial, and thermodynamic descriptors were generated with the QSAR+ module of Cerius^2 (CHARMm, Gasteiger, MOPAC, CNDO, MNDO, and Hopfinger methods). Similar descriptors were also calculated with the PC chip-based program Molecular Modeling Pro (version 1.4) (WindowChem Software, Fairfield, CA), which uses a variety of simplified computational approaches (Del Re, Lyman, Kier and Hall, and Hansch and Leo).

Equation generation. The genetic function approximation algorithm (Hahn and Rogers, 1995; Rogers and Hopfinger, 1994) was implemented for three different collections of structures/receptors/descriptors. In each case, the algorithm was set up to discover descriptor-activity relationships consisting of linear polynomial terms starting with 100 random initial equations with four variables, adding constants where necessary to search for equations of unlimited length but with acceptable lack-of-fit scores (Friedman, 1990). New "child" equations were generated using the least-squares regression method. Child equations were "mutated" (i. e., changed at "birth") 50% of the time after their generation by addition of randomly selected new terms. The number of generations of equation evolution required in each of the three data sets was gauged by the attainment of adjusted R^2 values and minimum lack-of-fit scores. Each data set required at least 20,000 generations before term usage reached a plateau. The equations were judged for statistical soundness by Friedman's lack-of-fit, R^2, adjusted R^2, F-test, least-squares error, and Mallow's C(p) statistics (Friedman, 1990; Hahn and Rogers, 1995; Rogers and Hopfinger, 1994).

Molecular superimpositions. Structural models of curacin A and the 26 analogs were constructed as described above and that for colchicine was built from the crystal coordinates (Lessinger and Margulis, 1978) with energy minimization as described previously (ter Haar *et al.*, 1996). These models will be described in Discussion. For compound superimposition to maximize atomic overlap, the rigid body fitting to target method was employed using a subgraph search routine, with the energy-minimized model of curacin A as the target. Rigid fitting rotates and translates the moving model with respect to the target so as to minimize the root-mean-square difference of the atom matches with the target with the root-mean-square difference defined as follows:

$$\left(\sum_{J=1}^{n} d_{J,J'}{}^2 \div n \right)^{1/2}$$

where $d_{J,J'}$ is the distance between the Jth matched atoms. The subgraph search routine treats each model as a graph with labeled nodes and edges. It finds the largest subgraph contained by the target and moving molecules.

Results

Functional Structure-Activity Studies

In the studies that follow, we compared 26 available analogs with curacin A as inhibitors of tubulin assembly and of colchicine binding to tubulin. In the colchicine binding assay, all analogs were initially examined at an equimolar concentration with the colchicine (5 μM). Analogs showing minimal inhibitory effect at this low concentration were also evaluated in 10-fold molar excess to detect weaker inhibitory activity. Finally, the 26 analogs were compared with curacin A for inhibitory effects on the growth of MCF-7 breast cancer cells.

Modifications in the backbone of the 14-carbon side chain. Previously, we had described the activities of partially purified curacins B and C and reported that compound **1** (C15–16 olefinic bond reduced) had activities similar to those of curacin A (Blokhin *et al.*, 1995). The successful resolution of the two natural products (Yoo and Gerwick, 1995) led us to reevaluate them, along with compound **1** and compound **2**, in which both the C3–4 and C15–16 olefinic bonds are reduced (Table 1).

Curacin B, with an *E*-to-*Z* transition at the C7–8 olefinic bond, and compound **1** differed little from curacin A in their interactions with tubulin. Both compounds strongly inhibited tubulin assembly and colchicine binding. Although compound **1** was equivalent to curacin A as an inhibitor of the growth of MCF-7 breast carcinoma cells, curacin B was almost 10-fold less active.

Curacin C, with an *E*-to-*Z* transition at the C9–10 olefinic bond, and compound **2** were significantly less active than curacin A in all assays. As inhibitors of assembly, they had IC_{50} values 3- and 6-fold higher, and they only weakly inhibited the binding of colchicine to tubulin. They were almost 100-fold less effective than curacin A as inhibitors of MCF-7 cell growth.

Modifications in the side chain substituents at C10 and C13. Curacin D differs structurally from curacin A only in lacking the C10 methyl substituent. It was almost 7-fold less active than curacin A as an inhibitor of tubulin assembly (similar in potency to compound **2**), but it remained a strong inhibitor of the binding of colchicine to tubulin, similar in potency to curacin B. Its antiproliferative activity was also similar to that of curacin B, in that it was almost 10-fold less potent than curacin A with MCF-7 cells.

The remaining compounds presented in Table 2 are modified in the C13 substituent. Compound **3** has reversal of configuration (*S* rather than *R*) at this position, compound **4** is the demethyl derivative, and compounds **5**-**8** bear different substituents. Compound **6** is notable in having an ethylenediether bridge at this position, representing conversion of C13 to a nonchiral position.

Reversal of configuration at C13 had little effect in the systems we examined. Like curacin A, compound **3** potently inhibited tubulin assembly and binding of [^{3}H]colchicine to tubulin, and it was only about 5-fold less active as an inhibitor of MCF-7 cell growth.

Demethylation of the C13 substituent (compound **4**) produced an agent almost indistinguishable from curacin A in the biochemical assays. Compound **4**, however, was about 12-fold less active as an inhibitor of MCF-7 cell growth.

Replacement of the methyl group at C13 had variable effects. Compound **5**, with a methoxymethyl group replacing the methyl group, had activity essentially indistinguishable from that of 13*S*-curacin A (compound **3**), with reversal of configuration at C13. Compound **6**, with an ethylenedioxy bridge at C13 causing loss of chirality, was equivalent to curacin A in all systems, including perhaps slightly greater potency as an inhibitor of MCF-7 cell growth. Bulky groups at the C13 oxygen, however, yielded compounds with little activity. A fluorinated butyl group (compound 7) yielded a compound with relatively weak inhibitory activity in both the polymerization and colchicine binding assays, and a benzoyl group (compound **8**) resulted in an agent inert in all assays.

Modifications in the thiazoline ring. Three compounds can be considered as representing modifications in the thiazoline moiety of curacin A. In compound **9**, configuration is reversed at position C2 (changed from *R* to *S*). In compound **10**, the C1–2 bond is oxidized, changing the ring to a thiazole ring. In compound **11**, an acetyl group was introduced at the C2 nitrogen, resulting in the disruption of the thiazoline ring (Table 3).

Of these modifications, the smallest effect was observed with oxidation of the C1–2 bond. Compound **10** had activities in the tubulin assays equivalent to those of curacin A, and it was 8-fold less potent as an inhibitor of MCF-7 cell growth. Compound **11**, with the disrupted thiazoline ring, was half as active as curacin A as an inhibitor of tubulin assembly, but it only weakly inhibited colchicine binding. Compound **9**, with reversal of configuration at C2, was a weak inhibitor of assembly (one eighth as active as curacin A) and colchicine binding. Compounds **9** and **11** had limited activity as inhibitors of MCF-7 cell growth.

Modifications in the cyclopropyl ring. Three compounds can be considered as representing modifications in the cyclopropyl moiety of curacin A. In compound **12** configuration is reversed at position C19 (changed from *R* to *S*). In compound **13** configuration is reversed at position C21 (changed from *S* to *R*). In compound **14** the cyclopropyl ring was disrupted by heat treatment (Table 4).

Compared with the analogous changes in the thiazoline ring (reversal of configuration; ring disruption), the modifications in compounds **12**-**14** caused only minor changes in analog activity relative to curacin A. The activities of compound **12** (19*S*-curacin A) were almost indistinguishable from those of curacin A. Disruption of the cyclopropyl ring (compound **14**) resulted in less loss of activity than reversal of configuration at C21 (compound **13**, 21*R*-curacin A). Nevertheless, both **13** and **14** were reasonably good inhibitors of assembly and colchicine binding, but they were 8–9-fold less potent than curacin A as inhibitors of MCF-7 cell growth.

Double and triple modifications. Six compounds (**15**–**20**) combine two of the modifications described above, and a seventh compound (**21**) has three modifications (Table 5). The results obtained with these agents are largely consistent with those obtained with the singly modified compounds.

Compound **15** combines C13 demethylation (compare with compound **4**) with reversal of configuration at C19 (compare with compound **12**). Compound **15** had activities in the tubulin assays comparable with those of curacin A, as had both **4** and **12**. Its activity against MCF-7 cells (IC_{50} = 0.61 μM) was slightly less than that of **4** (IC_{50} = 0.45 μM) and much less than that of **12** (IC_{50} = 0.09 μM).

Compound **16** has a methoxymethyl group replacing the C13 methoxy (compare with compound **5**) combined with reversal of configuration at C19 (compare with compound **12**). The doubly modified analog was less active in all assays than either of the singly modified analogs.

Compound **17** has a benzoate residue replacing the C13 methoxy (compare with compound **8**) combined with reversal of configuration at C19 (compare with compound **12**). Like compound **8**, **17** was inactive in all assays.

Compound **18** combines reversal of configuration at C13 (compare with compound **3**) and reversal of configuration at C19 (compare with compound **12**). As with **16**, the doubly

TABLE 1

Side chain backbone modifications

In the colchicine binding assay, inhibitor concentration was 5.0 μM, except for the values in parentheses, where the inhibitor concentration was 50 μM. Note that configuration at C13 is *R* in curacins B and C, as well as in curacin A. The α orientation in the diagrams of the methoxy substituent in curacins B and C is necessitated by the *E*-to-*Z* transition at the C7-8 and C9-10 olefinic bonds, respectively.

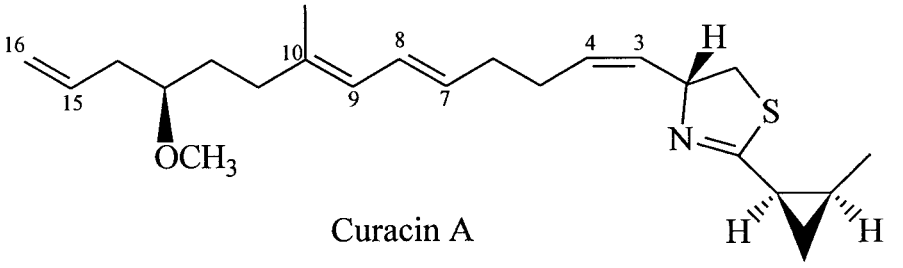

Curacin A

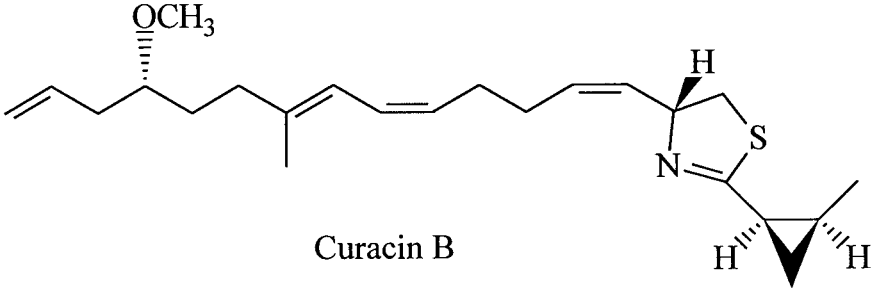

Curacin B

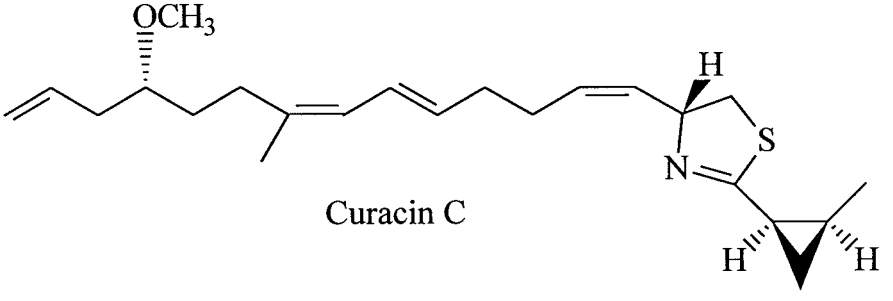

Curacin C

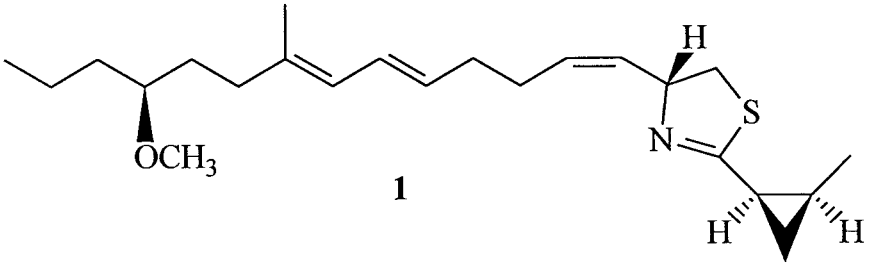

1

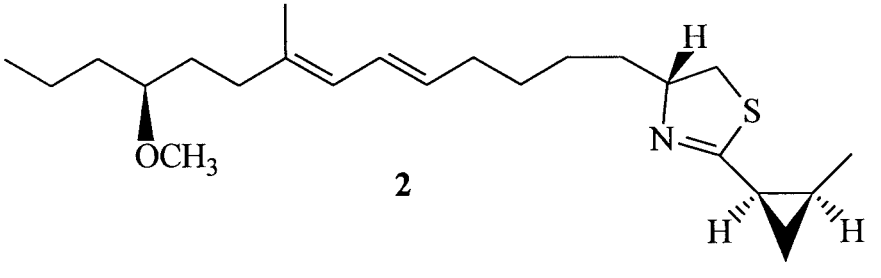

2

Compound	Inhibition of tubulin polymerization	Inhibition of colchicine binding	Inhibition of MCF-7 growth
	IC_{50} ± SD (μM)	*% inhibition ± SD*	*IC_{50} ± SD (μM)*
Curacin A	0.72 ± 0.2	94 ± 2	0.038 ± 0.01
Curacin B	0.82 ± 0.2	56 ± 2	0.32 ± 0.06
Curacin C	2.3 ± 1	10 ± 2 (50 ± 3)	3.6 ± 0.8
1	1.2 ± 0.2	85 ± 7	0.046 ± 0.01
2	4.6 ± 1	1 ± 1 (28 ± 6)	3.3 ± 2

SD, standard deviation.

TABLE 2
Side chain substituent modifications
In the colchicine binding assay, inhibitor concentration was 5.0 μM, except for the values in parentheses, where the inhibitor concentration was 50 μM.

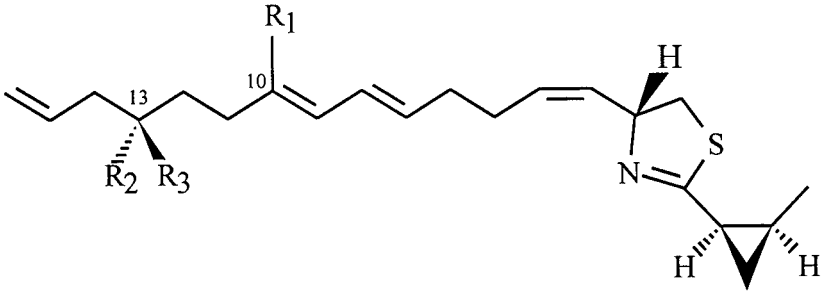

Compound	R_1	R_2	R_3	Inhibition of tubulin polymerization	Inhibition of colchicine binding	Inhibition of MCF-7 growth
				IC_{50} ± SD (μM)	*% inhibition ± SD*	*IC_{50} ± SD (μM)*
Curacin A	CH_3	H	OCH_3	0.72 ± 0.2	94 ± 2	0.038 ± 0.01
Curacin D	H	H	OCH_3	4.8 ± 0.4	53 ± 10	0.34 ± 0.1
3	CH_3	OCH_3	H	0.67 ± 0.2	56 ± 6	0.18 ± 0.02
4	CH_3	H	OH	0.87 ± 0.09	82 ± 7	0.45 ± 0.02
5	CH_3	H	OCH_2OCH_3	0.64 ± 0.2	81 ± 6	0.22 ± 0.02
6	CH_3	OCH_2CH_2O		0.78 ± 0.3	92 ± 1	0.030 ± 0.01
7	CH_3	H	$OCH_2(CF_2)_2CF_3$	5.4 ± 1	12 ± 4 (29 ± 9)	>10
8	CH_3	H	$OCOC_6H_5$	>80	5 ± 5 (2 ± 4)	>10

SD, standard deviation.

modified **18** was less active in all assays than either of the singly modified analogs.

Compound **19** combines reversal of configuration at C2 (compare with compound **9**) and reversal of configuration at C19 (compare with compound **12**). With **19**, inhibition of tubulin assembly and colchicine binding were closer to the stronger activity of **12** than to the weaker activity of **9**. However, **19** was more like **9** than **12** in its minimal ability to inhibit the growth of MCF-7 cells.

Compound **20** combines reversal of configuration at C13 (compare with compound **3**) with reversal of configuration at C21 (compare with compound **13**). As compound **20** was almost inert, it was substantially less active than the singly modified analogs, which is somewhat similar to the situation with compounds **16** and **18**. These latter compounds had, however, retained significant activity as inhibitors of tubulin assembly.

Compound **21** combines reversal of configuration at C2 (compare with compound **9**), reversal of configuration at C19 (compare with compound **12**), and reversal of configuration at C21 (compare with compound **13**). The activities of compound **21** most closely resembled those of **13**, which was more active than **9** and less active than **12**.

Partial structures. Two available compounds represent incomplete curacin A structures (Table 6). Compound **22** is a C4 through C16 segment of curacin A used as a synthetic precursor (White *et al.*, 1997). It was essentially inactive in all assays. Compound **23**, formed in a degradative reaction from compound **11**, contains the entire side chain together with a disrupted thiazoline ring, but it completely lacks the cyclopropyl residue. Compound **23** has significant activity as an inhibitor of tubulin assembly, being about half as active as compound **11**. It also is a weak inhibitor of colchicine binding to tubulin and seemed to be somewhat more active than compound **11**. Like compound **11**, compound **23** only feebly inhibits the growth of MCF-7 cells.

Accumulation of MCF-7 Cells with G2/M DNA Content after Treatment with Curacin A Analogs

As will be described below (see Discussion), there was a relatively poor correlation between a drug's inhibition of tubulin polymerization and its inhibitory effects on MCF-7 cell growth. This could be a consequence of different mechanisms of action with different compounds in drug-treated cells. We showed previously that after treatment of cells with curacin A, both the mitotic index and the proportion of cells with G2/M DNA content increased as the drug concentration rose (Gerwick *et al.*, 1994). We therefore compared the effects of curacin A and several analogs that strongly inhibited assembly but with widely divergent IC_{50} values for cell growth on the accumulation of MCF-7 cells with G2/M DNA content (Fig. 2). Despite their differing effects on cell growth, compounds **3**, **4**, and **21** all showed a close correlation between cytotoxicity and accumulation of cells with tetraploid DNA. This strongly indicates that all the active analogs have the same cellular mechanism of action as curacin A.

QSAR Molecular Modeling Studies

A computational approach was employed in an attempt to develop QSAR equations that would explain relative analog activities as inhibitors of polymerization, colchicine binding, and/or MCF-7 cell growth in physicochemical and/or linear free energy terms. Such an analysis could provide insight useful for additional synthetic efforts. Three independent QSAR calculations based on the experimental data were performed. In each analysis, structures were superimposed on the most active congener (compound **5** for polymerization, **6** for cell growth, curacin A itself for colchicine binding), and "receptor" models were generated with the activity of each structure weighting its contribution to the respective model. A set of 65 electronic shape, spatial, thermodynamic, and "receptor"-derived energy descriptors were calculated with algorithms contained in the Cerius[2]

TABLE 3
Thiazoline ring modifications
In the colchicine binding assay, inhibitor concentration was 5.0 μM, except for the values in parentheses, where the inhibitor concentration was 50 μM.

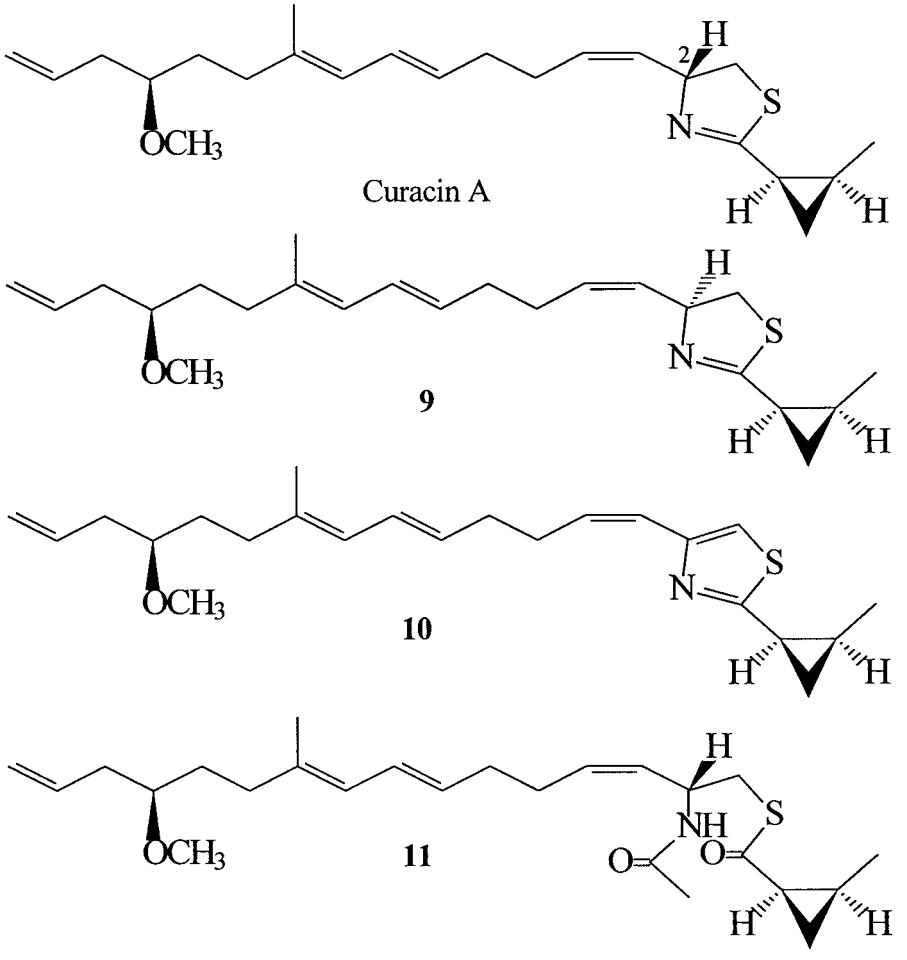

Compound	Inhibition of tubulin polymerization	Inhibition of colchicine binding	Inhibition of MCF-7 growth
	IC_{50} ± SD (μM)	*% inhibition ± SD*	*IC_{50} ± SD (μM)*
Curacin A	0.72 ± 0.2	94 ± 2	0.038 ± 0.01
9	5.5 ± 0.7	3 ± 5 (50 ± 6)	>1[a]
10	0.74 ± 0.01	74 ± 11	0.30 ± 0.07
11	1.5 ± 0.4	9 ± 8 (32 ± 2)	4.2 ± 2

[a] Insufficient sample to test at higher concentrations.
SD, standard deviation.

and Molecular Modeling Pro suites of computational chemistry programs for each curacin derivative for each of the three analyses.

Because the calculated descriptors far outnumbered the curacin derivatives, a method specifically designed for such unbalanced data sets, the genetic function approximation algorithm (Hahn and Rogers, 1995; Rogers and Hopfinger, 1994), was employed to generate statistically valid equations for the three biological activities. Acceptance of an equation required appropriate statistical measures: adjusted $R^2 > 0.67$; F-statistic > 9.0; Mallow's C(p) < - 2.0; Friedman's lack-of-fit < 1.0.

For the tubulin polymerization inhibition data set, the equation with the greatest statistical significance that was found was:

$$-(\log IC_{50}) = 9.061 + (3.006)(XDIP) - (0.6801)(Log\ P) - (0.0599)(\kappa 2) - (78.8776)(LUMO) + 7.9926(d) \quad (1)$$

where XDIP is the calculated measure of the *x*-contribution to dipole moment; κ2 is the calculated shape index from Kier and Hall's graph theory methods (Kier and Hall, 1986); LUMO is the calculated energy level of the lowest unoccupied molecular orbital [calculated mainly by Del Re's method (Del Re, 1958) as implemented in Molecular Modeling Pro, but some calculations according to CNDO and/or MNDO partial charge terms were added for reasonable accuracy]; Log P is the log of the calculated 1-octanol-water partition coefficient; and *d* is the calculated density of the compound. The statistical parameters for eq. 1 were as follows: $R^2 = 0.776$; adjusted $R^2 = 0.706$; F-test = 11.082; least-squares error = 0.108; Mallows C(p) = - 9.711; Friedman's lack-of-fit score = 0.363.

A single descriptor in eq. 1 showed a linear trend in relation to biological activity. This was the XDIP. In general, the higher the XDIP, the more the compound inhibited tubulin assembly. Compound **5** had the highest XDIP value, at 0.259

TABLE 4
Cyclopropyl ring modifications
In the colchicine binding assay, inhibitor concentration was 5.0 μM.

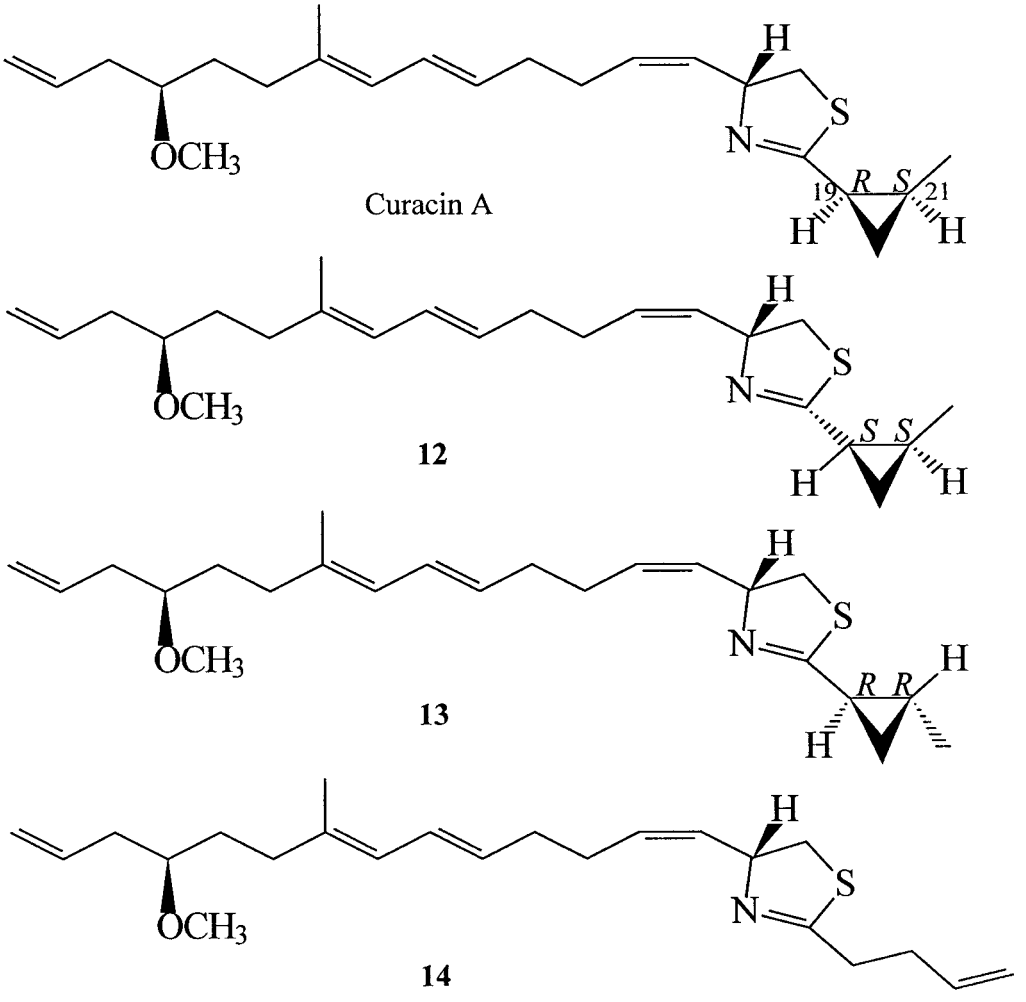

Compound	Inhibition of tubulin polymerization	Inhibition of colchicine binding	Inhibition of MCF-7 growth
	IC_{50} ± SD (μM)	% inhibition ± SD	IC_{50} ± SD (μM)
Curacin A	0.72 ± 0.2	94 ± 2	0.038 ± 0.01
12	0.77 ± 0.2	88 ± 11	0.090 ± 0.01
13	2.1 ± 0.5	48 ± 5	0.36 ± 0.09
14	0.92 ± 0.2	83 ± 6	0.30 ± 0.2

SD, standard deviation.

D, and compounds **3** and **6** and curacin A had values > 0.100 D. In contrast, the inactive fluorinated compound **7** had the lowest value, at - 0.376 D. None of the other descriptors in eq. 1 showed obvious linear trends when plotted against activity but were required to "fine-tune" the equation.

The MCF-7 growth inhibition data set was less amenable to QSAR analysis. Only one equation was found that met the statistical constraints:

$$-(\log IC_{50}) = -1.1967 - (0.2413(Dp) + (6.5580)(XDIP) + (9.82901)(d) + (0.5343)(Sr) + 1.0310(ZDIP) \quad (2)$$

where, besides the terms defined above, Dp is the calculated measure of molecular depth (z-coordinate); Sr is the calculated measure of superdelocalizability; and ZDIP is the calculated measure of the *z*-contribution to dipole moment. The statistical parameters for eq. 2 were as follows: $R^2 = 0.751$; adjusted $R^2 = 0.674$; F-test = 9.677; least-squares error = 0.152; Mallows C(p) = - 2.539; Friedman's lack-of-fit score = 0.511.

Again, the only descriptor with any linear trend, when plotted against inhibition of cell growth, was the XDIP. Overall, the correlation observed was similar to that obtained with the tubulin assembly data. For these equations, we should note that the dipole moment and its *x*, *y*, and *z* components were estimated from partial atomic charges (largely CHARMm charging rules) and atomic coordinates. Dipole properties may be correlated with long-range ligand-target recognition and binding (Hopfinger, 1973). It is as yet unclear how the *x*-component of the dipole moment may be easily manipulated by substitutions on the curacin backbone, but both our biological and computational findings clearly indicate that highly electronegative substituents near the C16

TABLE 5
Multiple modifications
In the colchicine binding assay, inhibitor concentration was 5.0 μM, except for the values in parentheses, where the inhibitor concentration was 50 μM.

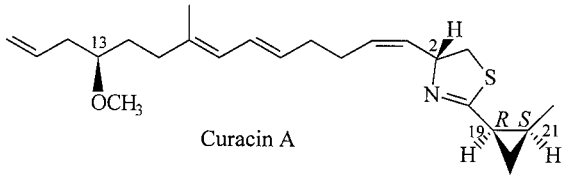

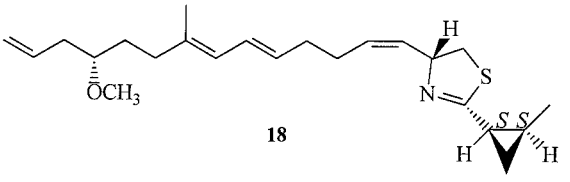

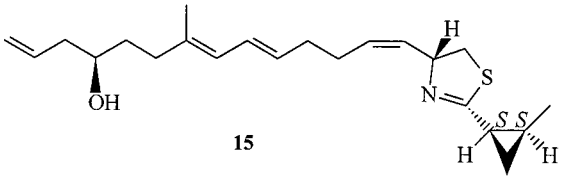

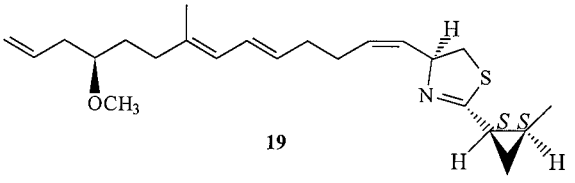

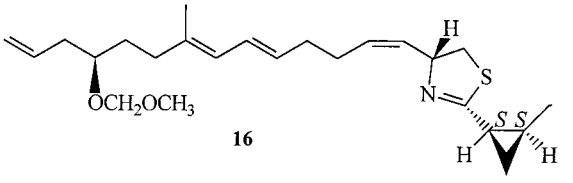

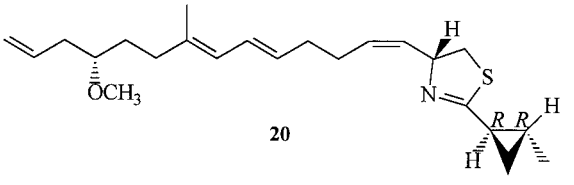

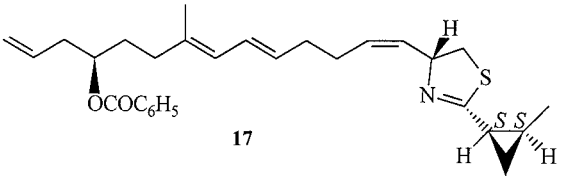

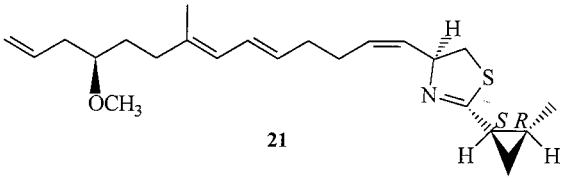

Compound	Inhibition of tubulin polymerization	Inhibition of colchicine binding	Inhibition of MCF-7 growth
	IC_{50} ± SD (μM)	% inhibition ± SD	IC_{50} ± SD (μM)
Curacin A	0.72 ± 0.2	94 ± 2	0.038 ± 0.01
15	0.73 ± 0.1	71 ± 5	0.61 ± 0.2
16	3.2 ± 0.3	16 ± 3 (32 ± 4)	3.1 ± 2
17	>80	7 ± 4 (2 ± 3)	>10
18	5.5 ± 0.7	2 ± 2 (39 ± 4)	>1[a]
19	1.1 ± 0.08	41 ± 4	2.2 ± 0.6
20	40 ± 10	4 ± 1 (4 ± 5)	>10
21	1.9 ± 0.1	23 ± 11 (85 ± 3)	0.45 ± 0.09

[a] Insufficient sample to test at higher concentrations.
SD, standard deviation.

end of the hydrocarbon backbone should result in substantial loss of activity.

No statistically valid equation was found to describe the colchicine binding inhibition data set. This probably results from the limited studies performed thus far (evaluation of inhibitory effects at only one or two curacin analog concentrations).

Our overall conclusion from the above analysis is that more refined QSAR formulas that can reliably predict relative activity of new structures will require preparation and analysis of additional curacin derivatives, especially compounds containing greater structural diversity. In this regard, we should also note that an insufficient number of analogs modified at C13 are currently available to perform a quantitative Hansch analysis (Hansch and Leo, 1979) of substituent effects on compound activity.

Discussion

Functional structure-activity analysis of the interaction of curacin A with tubulin. We compared natural and synthetic curacin A with each other and with 26 structural analogs, including three natural products, as inhibitors of tubulin assembly and of the binding of colchicine to tubulin. In general, the results from these two assays were in excellent agreement with each other.

The assembly reaction was performed under a suboptimal reaction condition, made necessary because curacin A induces formation of complex aggregates of twisted cables of fine spiral filaments (Hamel *et al.*, 1995). Under optimal assembly reaction conditions, we were unable to identify a curacin A concentration that inhibited turbidity development by 50%, but under the reaction condition used here,

TABLE 6

Partial structures

In the colchicine binding assay, inhibitor concentration was 5.0 μM, except for the values in parentheses, where the inhibitor concentration was 0 μM.

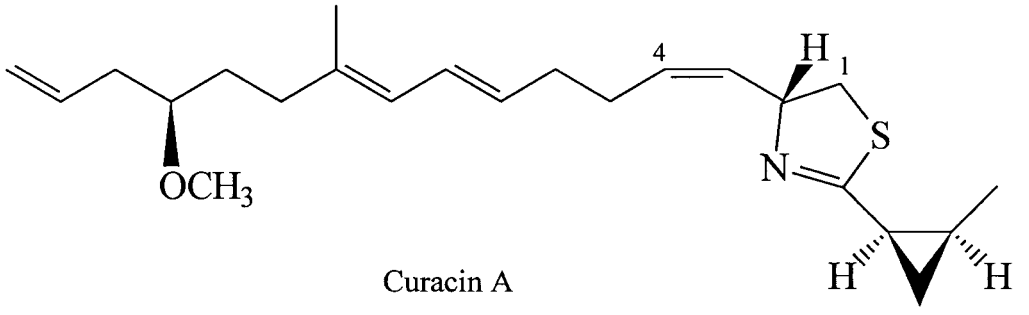

Curacin A

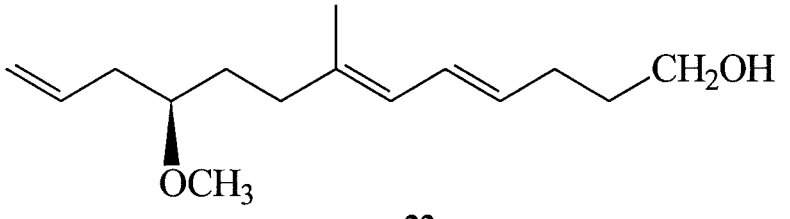

22

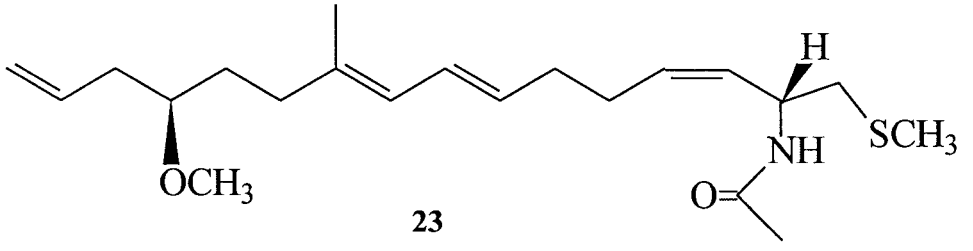

23

Compound	Inhibition of tubulin polymerization	Inhibition of colchicine binding	Inhibition of MCF-7 growth
	IC_{50} ± SD (μM)	*% inhibition ± SD*	*IC_{50} ± SD (μM)*
Curacin A	0.72 ± 0.2	94 ± 2	0.038 ± 0.01
22	>80	0[a] (5 ± 4)	>10
23	3.3 ± 0.8	12 ± 15 (67 ± 11)	5.2 ± 3

[a] The same value was obtained in three experiments.

turbidity development disappeared with substoichiometric concentrations of curacin A before reappearing with a stoichiometric concentration.

The colchicine binding assay was performed under near-optimal reaction conditions (Hamel and Lin, 1981), and at the incubation time selected the control reaction was about 50% complete. Because curacin A is so potent an inhibitor of colchicine binding (Blokhin *et al.*, 1995), this series of compounds was examined with equimolar inhibitor and colchicine, with the drugs in 5-fold molar excess over tubulin.

Despite these differences, every analog that yielded an assembly IC_{50} value below 1.0 μM inhibited colchicine binding by over 50%; conversely, most compounds with assembly IC_{50} values over 1.0 μM were weak inhibitors of colchicine binding. Two major exceptions to this generalization were compound **1** (1.2 μM assembly IC_{50}, 85% colchicine binding inhibition) and curacin D (4.8 μM assembly IC_{50}, 53% colchicine binding inhibition). At the opposite extreme, four analogs (**8**, **17**, **20**, and **22**) had minimal activity in both assays.

Relatively little impact on the tubulin-drug interaction was observed with some side chain backbone modifications (reduction of the C15–16 olefinic bond; *E*-to-*Z* transition of the C7–8 olefinic bond), major modifications in the C13 substituent, oxidation of the C1–2 bond in the thiazoline ring, and major changes in the cyclopropyl ring (its disruption or reversal of configuration at C19). The strong inhibition of colchicine binding by curacin D suggests that the C10 methyl group is not important in the drug-tubulin interaction, but the reduced activity of curacin D as an inhibitor of assembly makes this conclusion uncertain. In addition, reversal of configuration at both C19 and C21 of the cyclopropyl moiety yielded a compound with moderate loss of inhibitory activity in both the assembly and colchicine binding assays (compound **13**).

Significant loss of activity, especially in terms of reduced inhibition of colchicine binding, occurred with other side chain backbone changes (*E*-to-*Z* transition of the C9–10 olefinic bond and, probably, reduction of the C3–4 olefinic bond, although the latter was not available as an isolated modification of the molecule), changes in the thiazoline moiety (reversal of configuration at C2 and disruption of the thiazoline ring), bulky substituents replacing the C13 methoxy group, and truncation of the molecule (the inactive compound

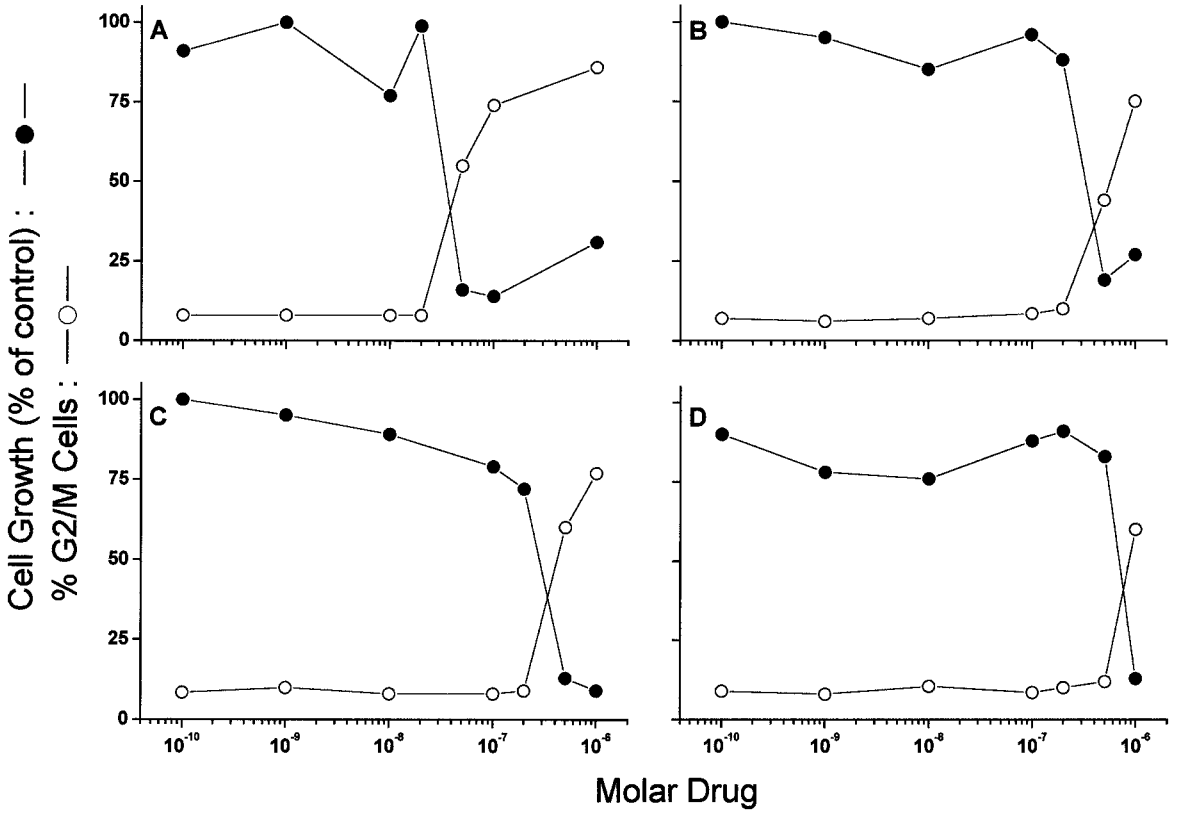

Fig. 2. Effects of curacin A (A) and compounds **3** (B), **4** (C), and **21** (D) on the proportion of MCF-7 cells with G2/M DNA content in comparison with drug effects on cell growth. Cells were treated for 48 hr with the indicated drug concentrations and quantified for cell growth and G2/M arrest as described in the text.

22 represents a segment spanning C4-C16 and the weakly active compound **23** contains the entire side chain and a portion of the thiazoline ring).

Reversal of configuration at C13 and demethylation had negligible effects on the interaction of curacin A with tubulin. It thus seems unlikely that the C13 methoxy group is a major recognition feature for tubulin in its interaction with curacin A. Further, compound **6**, with an ethylenedioxy bridge doubly attached at C13, has no chiral asymmetry at that position and is fully active. Similarly, replacement of the methyl group with the relatively small methoxymethyl residue yielded an active compound, while bulkier groups yielded poorly active (compound **7**) or inactive (compound **8**) agents.

These effects at C13 are reminiscent of certain structure-activity findings with both colchicine and podophyllotoxin (reviewed in Hamel, 1990). With colchicine, the C7 side chain is not essential for activity. Moreover, a wide variety of substituents are found in active analogs, but very bulky derivatives reduce or eliminate activity. Even the well known requirement for *S* configuration at C7 has been attributed to an effect on biaryl configuration rather than configuration at C7 *per se*. With podophyllotoxin, configuration at C4 is not important for activity, except that bulky groups in epipodophyllotoxin derivatives eliminate the drug-tubulin interaction.

In summary, the most important portions of curacin A required for its interaction with tubulin are the thiazoline ring and the side chain at least through C4, the portion of the side chain including the C9–10 olefinic bond, and, perhaps, the C10 methyl group. Nevertheless, only two modifications among those we have examined totally eliminate the tubulin-drug interaction. The exceptions are a benzoate residue at C13 and the C4-C16 segment represented by compound **22**. Minimal activity was also observed with compound **20**, which combined two modifications that alone had minor effects on analog activity.

These conclusions are in agreement with the findings of Onoda *et al.* (1996b). These researchers found compound **22** to be inactive as an inhibitor of assembly of microtubule protein (tubulin unresolved from microtubule-associated proteins). They further demonstrated that the two segments shown in Fig. 3 were inactive.

The strong activity in all assays, especially with MCF-7 cells, of compounds **1** and **6** indicates that the C13 substituent and the C15–16 olefin bond, in particular, merit further synthetic exploration in a search for more potent and/or more soluble analogs.

Comparison of inhibitory effects on MCF-7 cell growth with effects on the drug-tubulin interaction. We examined the curacin A analogs for inhibitory effects on the growth of the MCF-7 cell line, as it was one of the lines in the NCI 60-cell line panel (Monks *et al.*, 1991) with greatest sensitivity to curacin A. From the data in Tables 1–6, it is

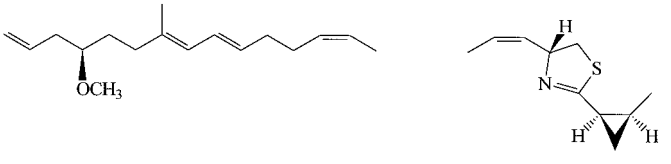

Fig. 3. Inactive segments of curacin A (Onoda *et al.*, 1996b).

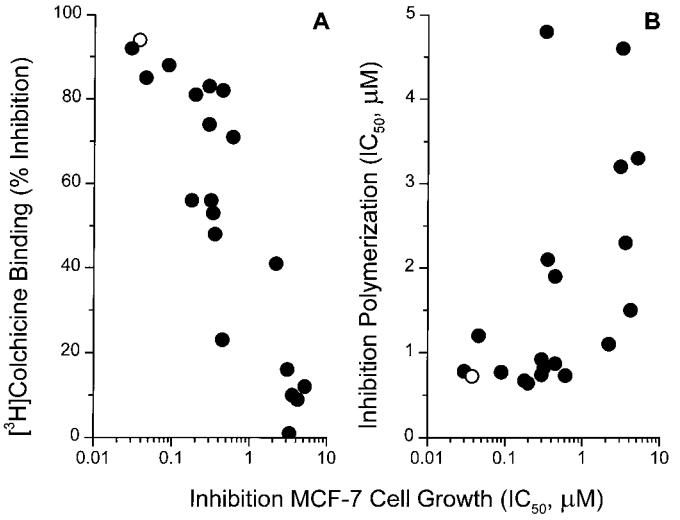

Fig. 4. Correlation of antiproliferative and antitubulin activities of curacin A analogs. A. Inhibition of MCF-7 cell growth versus inhibition of colchicine binding. B. Inhibition of MCF-7 cell growth versus inhibition of tubulin polymerization. The data presented in Tables 1–6 are shown. ●, different compounds; ○, curacin A. Compounds for which no IC_{50} value for cell growth was obtained are not shown. For panel A, the correlation coefficient is 0.997. For panel B, the best correlation coefficient (0.500) was obtained when the data were plotted in a log/log format.

clear that we were not successful in modifying curacin A to yield an agent significantly more potent against the MCF-7 cells, and most analogs were less active. Two compounds (**1** and **6**) were essentially equivalent to curacin A, and one additional compound (**12**) was nearly as active.

Our initial impression, therefore, was that there would be little correlation between analog effects on cell growth and on analog interactions with tubulin, since nine analogs were potent inhibitors of polymerization ($IC_{50} < 1$ μM) and eleven were potent inhibitors of colchicine binding (>50% inhibition when equimolar with colchicine). However, there was a clear correlation between inhibition of colchicine binding and antiproliferative activity among these compounds (Fig. 4A). Compounds with IC_{50} values for cell growth below 0.1 μM all inhibited colchicine binding by at least 85%. On the other hand, compounds that were nearly as potent in their inhibitory effects on colchicine binding (71–83% inhibition) had IC_{50} values with the MCF-7 cells of 0.22–0.45 μM, perhaps limiting the predictive value of the colchicine binding assay. It is possible that modification of reaction conditions will enhance the utility of the assay as a primary screen for curacin A analogs. This is particularly important because the polymerization assay clearly did not predict antiproliferative activity (Fig. 4B). The potent assembly inhibitors had IC_{50} values with the MCF-7 cells that ranged from 0.030 to 0.61 μM.

Nevertheless, although an interaction with tubulin does not reliably predict antiproliferative activity with curacin A analogs, failure to strongly inhibit tubulin assembly and colchicine binding was invariably associated with limited effects on cell growth. All compounds with assembly IC_{50} values over 2 μM *and* colchicine inhibition values less than 20% (5 μM inhibitor) had IC_{50} values over 1 μM with MCF-7 cells. Moreover, despite quantitative differences in cytotoxic activity, all analogs examined, like curacin A, caused accumulation of MCF-7 cells in G2/M at concentrations that caused growth arrest. This strongly implies that differences in effects on cell growth derive from differences in drug uptake, retention, and/or metabolism by the cells or from differences in compound stability in tissue culture medium rather than from a different (nontubulin-based) mechanism of action.

Molecular superimposition modeling studies. Computer-driven molecular modeling, based on an energy minimization program, was used to generate the structural model of curacin A (shown in green) displayed in Figs. 5–7. This was done in an attempt to gain understanding of (a) the differential activity of the analogs and (b) the common structural features shared by curacin A and colchicine to account for their common binding site on tubulin.

Because the QSAR analysis had been most successful with the polymerization inhibition data, the nine analogs most active in this assay ($IC_{50} < 1.0$ μM) were selected for the initial structural modeling studies (Fig. 5A). Superimposition of the models of these compounds on curacin A showed marked likeness among relative positioning of atoms in three dimensional space, with the exception of curacin B (Fig. 5A,

Fig. 5. A. Three-dimensional computer models of curacin A (predominantly *green*) superimposed with analogs having polymerization IC_{50} values under 1.0 μM (compounds **3**, **4**, **5**, **6**, **10**, **12**, **14**, and **15** and curacin B). *Arrows,* regions of curacin B deviating from the curacin A structure. B. Three dimensional computer models of curacin A (predominantly *green*) superimposed with all 26 analogs. The two best matches, compounds **3** and **5**, are shown predominantly in *rose* and *yellow*, respectively.

Fig. 6. Three-dimensional computer model comparisons of curacin A (*green*) with curacin B (*blue*) (A and C) or with curacin C (*red*) (B and D). The presentations are to demonstrate maximum overlap for each comparison. In A and B, maximum atom-to-atom matches were computer selected (subgraph search routine). The cyclopropyl and thiazoline moieties are on the *left* side of the diagrams. In C and D, these moieties were specifically matched, as described in the text, and are on the *right* side of the diagrams.

arrows). The other 17 analogs were then placed into the model (Fig. 5B), and most of the inactive analogs contained moieties that either fell outside the space occupied by curacin A or failed to occupy major regions of this space. Examples of such moieties in relatively inactive compounds are the phenyl groups of compounds **8** and **17**, the C15–16 olefin moiety and C10 methyl group of curacin C, and the fluorine atoms of compound **7**.

The contrast in activities between curacins B and C, with the former more comparable to curacin A than the latter in all bioassays, was particularly striking, since the structural model of neither compound superimposed well on that of curacin A (Fig. 6). [There also are major conformational differences between curacins B and C (direct comparison not presented).] The calculated intersection volumes of curacins B and C with curacin A are about 170 and 190 $Å^3$, respectively, about half of the total molecular volumes of about 380 $Å^3$. The computer-determined maximum overlap images are shown in Fig. 6A for curacin B and in Fig. 6B for curacin C. There is no obvious explanation in these models for the greater activity of curacin B versus curacin C.

Because the functional structure-activity studies clearly demonstrate the importance of the thiazoline ring and the C3–4 olefin group, both of which are present in curacins A, B, and C, along with the methyl-cyclopropyl moiety, we thought it worthwhile to manually overlay these portions of curacins B and C with curacin A. The results are shown in Fig. 6, C and D, for the curacin A/B and A/C comparisons, respectively. In terms of molecular overlap, there is again no ready explanation for the greater activity of curacin B relative to curacin C. These latter comparisons, however, do suggest that the greater interaction of curacin B with tubulin may derive from the less essential C6-C16 portion of the molecule projecting outside the binding site. In contrast, the C6-C16 portion of curacin C might hinder the overall interaction of the molecule with tubulin. The actual explanation for the different activities of the three natural products is most likely much more complex and may be resolved by analysis of additional analogs.

Finally, we have attempted to understand the structural analogies between curacin A and colchicine with computer-driven molecular modeling, by superimposing the structure of colchicine on that of curacin A (Fig. 7). There was only a 7-atom overlap, shown diagrammatically in Fig. 8. This rather minimal overlap region does include the most important structural features of curacin A identified in our studies (the thiazoline ring and the C3–4 olefin moiety), *but* five of these atoms in colchicine seem to be relatively unimportant for the interaction of the latter drug with tubulin. The bicy-

Fig. 7. Three-dimensional computer models showing the maximum atom-to-atom match of curacin A (*green*) with colchicine (*gray*), with oxygen atoms in *red*, the nitrogen atom in *blue*, and hydrogen atoms in *white*.

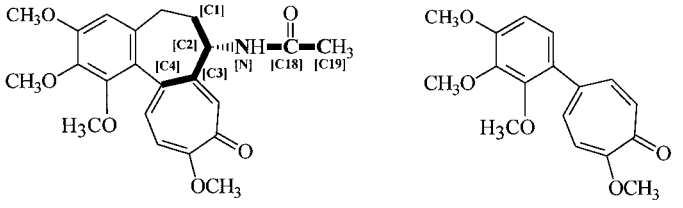

Fig. 8. Diagrams of colchicine (*left*) and 2-methoxy-5-(2′, 3′, 4′-trimethoxyphenyl)tropone (*right*). *Bold,* overlap atoms of colchicine with curacin A (see Fig. 7); *brackets*, corresponding atoms in curacin A (see Fig. 1 for position numbers).

clic analog 2-methoxy-5-(2′,3′,4′-trimethoxyphenyl)tropone, shown in Fig. 8, is an active colchicine analog, both in its interactions with tubulin and as an inhibitor of cell growth (Fitzgerald, 1976). On the other hand, the B ring of colchicine and its side chain have been shown to play a major role in the stability of the tubulin-colchicine complex (Banerjee *et al.*, 1987; Bhattacharyya *et al.*, 1986), and the structural analogies shown in Figs. 7 and 8 may account for the highly stable tubulin-curacin A complex (Blokhin *et al.*, 1995). We should also note that a computer-driven CASE/MultiCASE analysis of over 200 active colchicine site drugs identified over 20 drug biophores (specific atomic sequences) associated with interactions with tubulin (ter Haar *et al.*, 1996). None of these biophores are present in curacin A. Molecular modeling thus has not yet been able to reveal fully the specific structural analogies between curacin A and colchicine.

References

Banerjee A, Barnes LD, and Ludueña RF (1987) The role of the B-ring of colchicine in the stability of the colchicine-tubulin complex. *Biochim Biophys Acta* **913:**138–144.

Bhattacharyya B, Howard R, Maity SN, Brossi A, Sharma PN, and Wolff J (1986) B ring regulation of colchicine binding kinetics and fluorescence. *Proc Natl Acad Sci USA* **83:**2052–2055.

Blokhin AV, Yoo H-D, Geralds RS, Nagle DG, Gerwick WH, and Hamel E (1995) Characterization of the interaction of the marine cyanobacterial natural product curacin A with the colchicine site of tubulin and initial structure-activity studies with analogs. *Mol Pharmacol* **48:**523–531.

Del Re G (1958) A simple MO-LCAO method for the calculation of charge distributions in saturated organic molecules. *J Chem Soc* **:**4031–4040.

Fitzgerald TJ (1976) Molecular features of colchicine associated with antimitotic activity and inhibition of tubulin polymerization. *Biochem Pharmacol* **25:**1383–1387.

Friedman J (1990) Technical report no. 102. Laboratory for Computational Statistics, Department of Statistics, Stanford University, Stanford, CA.

Gerwick WH, Proteau PJ, Nagle DG, Hamel E, Blokhin A, and Slate DL (1994) Structure of curacin A, a novel antimitotic, antiproliferative, and brine shrimp toxic natural product from the marine cyanobacterium *Lyngbya majuscula. J Org Chem* **59:**1243–1245.

Hahn M and Rogers D (1995) Receptor surface models. 2. Application to quantitative structure-activity-relationships studies. *J Med Chem* **38:**2091–2102.

Hamel E (1990) Interactions of tubulin with small ligands in *Microtubule Proteins* (Avila J, ed) pp 89–191, CRC Press, Boca Raton, FL.

Hamel E (1996) Antimitotic natural products and their interactions with tubulin. *Med Res Rev* **16:**207–231.

Hamel E and Lin CM (1981) Stabilization of the colchicine-binding activity of tubulin by organic acids. *Biochim Biophys Acta* **675:**226–231.

Hamel E and Lin CM (1984) Separation of active tubulin and microtubule- associated proteins by ultracentrifugation and isolation of a component causing the formation of microtubule bundles. *Biochemistry* **23:**4173–4184.

Hamel E, Blokhin AV, Nagle DG, Yoo H-D, and Gerwick WH (1995) Limitations in the use of tubulin polymerization assays as a screen for the identification of new antimitotic agents: the potent marine natural product curacin A as an example. *Drug Dev Res* **34:**110–120.

Hansch C and Leo A (1979) *Substituent Constants for Correlation Analysis in Chemistry and Biology.* John Wiley and Sons, New York.

Hoemann MZ, Agrios KA, and Aubé J (1996) Total synthesis of curacin A. *Tetrahedron Lett* **37:**953–956.

Hopfinger AJ (1973) *Conformational Properties of Macromolecules.* Academic Press, New York.

Ito H, Imai N, Takao K, and Kobayashi S (1996) Enantioselective synthesis of curacin A. 2. Total synthesis of curacin A by condensation of C1–C7, C8- C17, and C18–C22 segments. *Tetrahedron Lett* **37:**1799–1800.

Kang G-J, Getahun Z, Muzaffar A, Brossi A, and Hamel E (1990) *N*-acetylcolchinol *O*-methyl ether and thiocolchicine, potent analogs of colchicine modified in the C ring: evaluation of the mechanistic basis for their enhanced biological properties. *J Biol Chem* **265:**10255–10259.

Kier LB and Hall LH (1986) *Molecular Connectivity in Structure-Activity Analysis.* John Wiley and Sons, New York.

Lai J-Y, Yu J, Mekonnen B, and Falck JR (1996) Synthesis of curacin A, an antimitotic cyclopropane-thiazoline from the marine cyanobacterium *Lyngbya majuscula. Tetrahedron Lett* **37:**7167–7170.

Lessinger L and Margulis TN (1978) The crystal structure of colchicine. A new application of magic integers to multiple-solution direct methods. *Acta Cryst* **B34:**578–584.

Ludueña RF and Roach MC (1991) Tubulin sulfhydryl groups as probes and targets for antimitotic and antimicrotubule agents. *Pharmacol Ther* **49:**133–152.

Ludueña RF, Prasad V, Roach MC, Banerjee M, Yoo H-D, and Gerwick WH (1997) Interaction of the cyanobacterial thiazoline-containing lipid curacin A with bovine brain tubulin. *Drug Dev Res* **40:**223–229.

Monks A, Scudiero D, Skehan P, Shoemaker R, Paull K, Vistica D, Hose C, Langley J, Cronise P, Vaigro-Wolff A, Gray-Goodrich M, Campbell H, Mayo J, and Boyd M (1991) Feasibility of a high-flux anticancer drug screen utilizing a diverse panel of human tumor cell lines in culture. *J Natl Cancer Inst* **83:**757–766.

Nagle DG, Geralds RS, Yoo H-D, Gerwick WH, Kim T-S, Nambu M, and White JD (1995) Absolute configuration of curacin A, a novel antimitotic agent from the tropical marine cyanobacterium *Lyngbya majuscula. Tetrahedron Lett* **36:**1189–1192.

Onoda T, Shirai R, Koiso Y, and Iwasaki S (1996a) Asymmetric total synthesis of curacin A. *Tetrahedron Lett* **37:**4397–4400.

Onoda T, Shirai R, Koiso Y, and Iwasaki S (1996b) Synthetic study of curacin A: a novel antimitotic agent from the cyanobacterium *Lyngbya majuscula. Tetrahedron* **52:**14543–14562.

Pack A, Jordan MA, Gerwick W, Jacobs RS, and Wilson L (1995) Curacin A, a new potent antimitotic marine natural product, increases dynamic instability of microtubules. *Proc Am Assoc Cancer Res* **36:**455.

Rogers D and Hopfinger AJ (1994) Application of genetic function approximation to quantitative structure-activity relationships and quantitative structure-property relationships. *J Chem Inf Comp Sci* **34:**854–866.

Skehan P, Storeng R, Scudiero D, Monks A, McMahon J, Vistica D, Warren JT, Bokesch H, Kenney S, and Boyd MR (1990) New colorimetric cytotoxicity assay for anticancer-drug screening. *J Natl Cancer Inst* **82:**1107–1112.

ter Haar E, Rosenkranz HS, Hamel E, and Day BW (1996) Computational and molecular modeling evaluation of the structural basis for tubulin polymerization inhibition by colchicine site agents. *Bioorg Med Chem* **4:**1659–1671.

White JD, Kim T-S, and Nambu M (1995) Synthesis of curacin A: a powerful antimitotic from the cyanobacterium *Lyngbya majuscula. J Am Chem Soc* **117:**5612–5613.

White JD, Kim T-S, and Nambu M (1997) Absolute configuration and total synthesis of (+)-curacin A, an antiproliferative agent from the cyanobacterium *Lyngbya majuscula. J Am Chem Soc* **119:**103–111.

Wilson L and Jordan MA (1995) Microtubule dynamics: taking aim at a moving target. *Chem Biol* **2:**569–573.

Wipf P and Xu W (1996) Total synthesis of the antimitotic marine natural product (+)-curacin A. *J Org Chem* **61:**6556–6562.

Yoo H-D and Gerwick WH (1995) Curacins B and C, new antimitotic natural products from the marine cyanobacterium *Lyngbya majuscula. J Nat Prod* **58:**1961–1965.

Send reprint requests to: Dr. E. Hamel, Building 37, Room 5D02, NIH, Bethesda, MD 20892-4255.